Highlights of Spanish Astrophysics XII, Proceedings of the XVI Scientific Meeting of the Spanish Astronomical Society held on July 15 - 19, 2024, in Granada, Spain. M. Manteiga, F. González Galindo, A. Labiano Ortega, M. Martínez González, N. Rea, M. Romero Gómez, A. Ulla Miguel, G. Yepes, C. Rodríguez López, A. Gómez García and C. Dafonte (eds.), 2025

Unveiling the central kpc of type I AGN in seeing-limited integral field spectroscopic data

García-Lorenzo, B.[1,2], Esparza-Arredondo, D.[1], Acosta-Pulido, J.[1,2], and Castro-Almazán, J.[1,2]

[1] Instituto de Astrofísica de Canarias, C/ Vía Láctea s/n, E-38205 La Laguna, Tenerife, Spain
[2] Departamento de Astrofísica, Universidad de La Laguna, E-38200 La Laguna, Tenerife, Spain

Abstract

We present an innovative deblending method that uses the variation of seeing with wavelength to isolate AGN and host galaxy spectra in IFS data. We demonstrate its efficacy through application to MUSE observations of the type I AGN MRK 926.

1 Introduction

The formation and evolution of galaxies result from a complex interplay between internal processes (e.g., nuclear activity, stellar feedback) and external factors (e.g., mergers), which shape their morphology and determine the scaling relations with their central supermassive black holes (SMBHs) [6]. Characterizing SMBHs and their host galaxies provides crucial constraints and insights into the co-growth scenario.

It is clear that SMBHs grow during active phases through gas accretion, observed as active galactic nuclei (AGN), which are classified based on accretion rates and the orientation of the accretion disk relative to the observer (e.g. [7]). At optical wavelengths, AGN spectra are classified into type-I and type-II based on the presence of broad and narrow emission lines, which arise from the Broad Line Region (BLR) on sub-parsec scales and from gas within the Narrow Line Region (NLR), extending several tens of parsecs, with a dusty torus separating the BLR from the NLR.

These active phases act as markers of co-evolution over cosmic time, as the presence of broad emission lines in AGN spectra enables us to measure the mass of the central SMBH in galaxies ranging from nearby to very distant using the single-epoch virial method (e.g. [5]). At the same time, the properties of the host galaxies (e.g., luminosity, size, morphology,

stellar velocity) should also be assessed accurately.

Integral field spectroscopic (IFS) observations of type-I AGN are particularly well-suited for exploring the cosmic evolution of the co-growth scenario. Data cube obtained from this observational technique may simultaneously reveal the mass of the central SMBH and the morpho-dynamics of their host galaxies. However, a significant challenge in studying the host galaxy of bright AGN over cosmic time using IFS is the contamination of the host galaxy's spectra by the light from the bright AGN, leading to a blend of their spectra.

In this work, we present an innovative deblending method specifically developed for seeing-limited IFS observations that uses the natural wavelength dependence of seeing (ϵ_0). This method effectively separates the light of the bright AGN from that of the host galaxy, allowing for an accurate analysis of both the central SMBH and the host galaxy properties. We demonstrate the efficacy of this approach through its application to MUSE observations of the type-I AGN MRK 926.

2 Methodology Description and Implementation

In seeing-limited IFS data, the AGN appears as a point-like source at the center of its host galaxy. If a model of the point spread function (PSF) were available for each wavelength, any point-like source, whether the AGN or a star in the field, could be effectively subtracted.

For type-I AGN, we can obtain an image of the PSF using the broad component of the emission lines characteristic of these active galaxies. Specifically, this can be achieved by recovering narrow-band filter images in spectral regions dominated by the AGN spectrum, such as those in the wings of the broad component of Hβ and Hα. A significant advancement would be to extend these PSFs from specific wavelengths into three dimensions (3D) across the entire spectral range, scaling the PSF flux to match the AGN's characteristics and subsequently subtracting it to isolate the spectra of the host galaxy.

In seeing-limited instruments, the largest variation of the PSF comes from atmospheric turbulence. Therefore, it is reasonable to use the dependence of atmospheric turbulence parameters to extend the PSF from a specific wavelength to other wavelengths (e.g. [4]). To validate this idea through the simultaneous implementation of the methodology, we utilized reduced data cubes from the Multi-Unit Spectroscopic Explorer (MUSE[1]) at the Paranal Observatory, operating in its seeing-limited mode, where atmospheric turbulence dominates the image quality (IQ) at the focal plane. The MUSE instrument spans the spectral range of ∼4750–9300 Å with a mean resolution of 3000 and spatially samples the sky using 0.2 arcsec spatial pixels.

Figure 1(a) presents an image of a bright nearby active galaxy. It is noteworthy that MUSE provides spectral information for each pixel in the observed field of view, where a few point-like sources are also present, some of which correspond to field stars. We selected one of these stars and defined about 50 narrow-band filters, each 40 Å wide, along the MUSE spectral axis, recovering the star's image in each filter (see Fig. 1 (b and c)). These images

[1]https://www.eso.org/sci/facilities/develop/instruments/muse.html

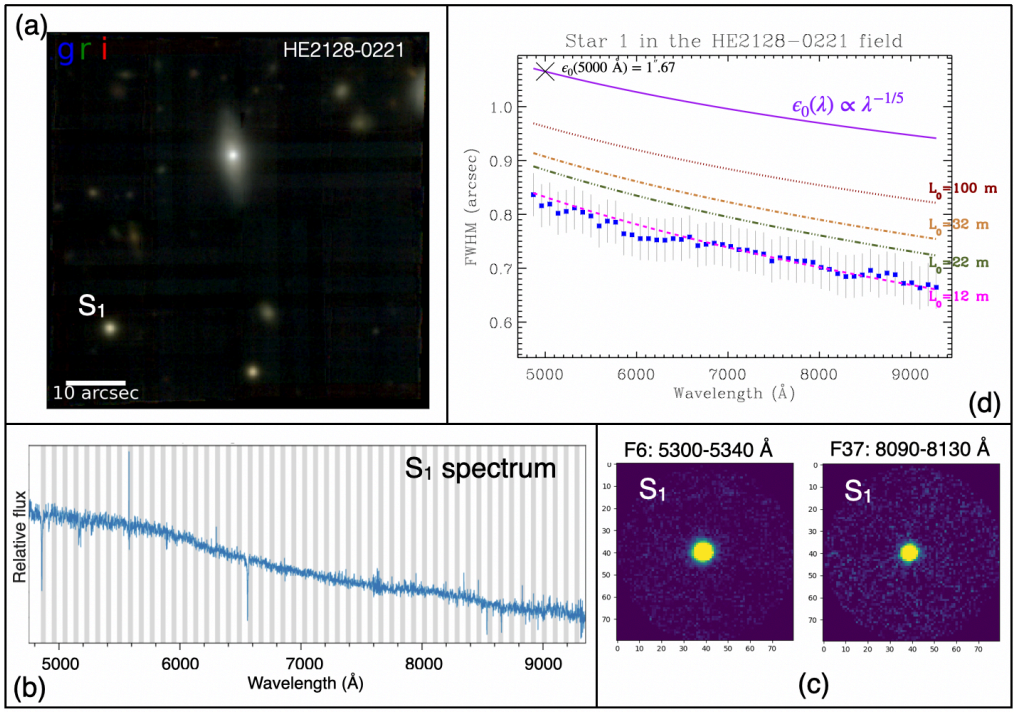

Figure 1: (a) Color-composite image recovered from MUSE observations of the active galaxy HE2128-0221. The MUSE field of view covers $\sim 60 \times 60$ arcsec^2 and shows several point-like sources, such as the star labeled S1. (b) Extracted spectrum within a 1-arcsec radius aperture from the MUSE data cube, centered on the peak of the S1 star. Vertical grey bands indicate the narrow-band filters selected to recover images of S1 at different wavelengths. (c) Two examples of narrow-band filter images of the S1 star, recovered by summing consecutive MUSE slices within the 5300–5340 Å and 8090–8130 Å spectral ranges (as labeled). (d) Wavelength dependence of the full width at half maximum (FWHM) for the Moffat fitting profile that quantifies the IQ (blue dots) of the S1 narrow-band filter images. The purple solid curve corresponds to the wavelength behavior of the ϵ_0 derived from the average seeing during the MUSE observations (i.e. 1.67 arcsecs at 5000 Å) indicated with a black X. Dashed-color curves correspond to the predicted IQ using equation 1 as a function of the wavelength for different values of the outer scales (as labeled): $\mathcal{L}_0$=100 → red, $\mathcal{L}_0$=32 → orange, $\mathcal{L}_0$=22 → olive green, and $\mathcal{L}_0$=12 → magenta.

were obtained under the same instrumental and atmospheric conditions, corresponding to the MUSE PSF at the equivalent wavelength of each narrow-band filter. Previous studies have shown that the MUSE PSF can be accurately modeled by a Moffat function with a power-law index of 2.5 (e.g. [1]). We therefore fitted the narrow-band filter images with an analytical Moffat profile using that power-law index and deriving the best-fitting parameters for each one.

Figure 1(d) shows the width of the Moffat profiles fitted to the 50 recovered narrow-band filter images as a function of wavelength. It also includes the spectral ϵ_0 variation (purple

line), showing that the image quality (IQ) at the MUSE focal plane is better than the DIMM seeing (ϵ_0) across all wavelengths. We found that the MUSE IQ is always better than expected based on the prevailing ϵ_0 conditions. Atmospheric optics concepts are essential to understand and explain these findings (see [4]).

While it is reasonable to expect that the final IQ is directly related to ϵ_0, following its theoretical wavelength dependence (assuming that instrumental aberrations and dome-seeing contributions are negligible), the limited size of the largest eddies in atmospheric turbulence, quantified by a parameter known as the outer scale ($\mathcal{L}_0$), smooths the expected image motion at the telescope's focal plane, thereby mitigating low spatial frequency perturbations. Consequently, the actual IQ at the focal plane will depend not only on ϵ_0 but also on $\mathcal{L}_0$, as described by Eq. 1 [8].

$$IQ(\lambda) \approx \epsilon_0(\lambda)\sqrt{1 - 2.183\left(\frac{0.976\lambda}{\epsilon_0(\lambda)\mathcal{L}_0}\right)^{0.356}} \tag{1}$$

Figure 1(d) presents the predicted IQ derived from Eq. 1 for various values of the outer scale, indicating that smaller outer scales correspond to better expected IQ at the focal plane. Using the prevailing ϵ_0 during the MUSE observations, it is evident that the measured IQ (blue squares in Fig. 1) closely aligns with the predicted IQ for an $\mathcal{L}_0$ of about 12 meters. The ϵ_0 values were retrieved from the differential image motion monitor (DIMM[2]) at the Paranal Observatory.

This test serves as empirical verification of the analytical equation for IQ(λ), suggesting that by imaging the IQ at a specific wavelength, we can use Eq. 1 to predict the IQ at different wavelengths, thereby allowing us to derive a 3D PSF model. This is exactly what we require in seeing-limited IFS of type I AGN: measurements of the IQ at particular narrow bands (associated with the broad component of emission lines) and a 3D-PSF to effectively remove the AGN contribution.

3 Application to deblend host and AGN spectra in MRK 926

Using the MUSE data cube for the type-I active galaxy MRK 926, we generated PSF images by selecting narrow-band filters in the wings of the broad Hβ and Hα components and subtracting a nearby continuum. These images were then modeled with Moffat profiles to derive the IQ at those narrow bands. We fitted the atmospheric function in Eq. 1 to determine the optimal combination of ϵ_0 and $\mathcal{L}_0$ that best matched those IQ measurements. Finally, we calculated the PSF for any slice within the MUSE spectral range using Eq. 1 and the retrieved ϵ_0 and $\mathcal{L}_0$, yielding a 3D-PSF normalized to a total flux of 1. Detailed descriptions of the methodology are provided in a forthcoming paper [3].

At this stage, a key step involves fitting the nuclear spectrum to isolate the point-like AGN contribution. To achieve this, we obtained a circular aperture spectrum of the galaxy centered on the AGN location. The radius of this aperture should be sufficiently large to

[2]http://archive.eso.org/wdb/wdb/asm/dimm_paranal/form

encompass nearly all the AGN flux while minimizing the contribution from the host galaxy. Testing with a model, we determined that a circular aperture with a radius of about five times the ϵ_0 provides a good compromise. Subsequently, we fitted the different components of this spectrum using QSFIT[2], a tool designed for fitting AGN spectra in the Sloan Digital Sky Survey archive. Finally, we scaled each slice of the 3D-PSF to the total flux of the fitted AGN contribution (including both the AGN continuum and broad components), resulting in a 3D spectrum of the isolated AGN. We are also exploring different approaches to account for the fraction of the narrow-line region (NLR) contributing to the unresolved nuclear spectrum; however, this step is not included in this discussion. For updates, please refer to [3].

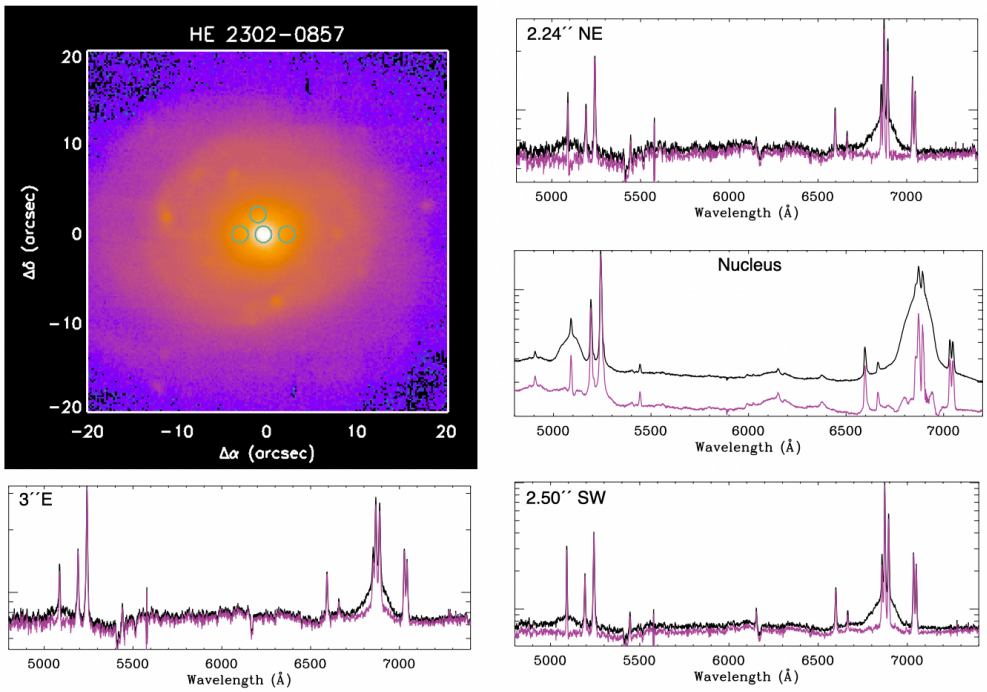

Figure 2: Recovered image of MRK 926 from the MUSE data after subtracting the 3D-PSF scaled to the AGN-pure spectrum. Four regions (green circles) are marked to indicate the circular apertures used to extract the spectra shown: before subtraction (black) and after subtraction (purple) of the AGN-scaled 3D-PSF. The labels in the spectra plot indicate the location of each aperture relative to the nucleus.

Figure 2 presents maps and spectra for MRK 926 before and after subtracting the AGN spectrum using our innovative method. The results we obtained are promising, enabling a detailed analysis of the circumnuclear region. Furthermore, the 3D-PSF derived from this innovative method, which takes advantage of atmospheric turbulence, could also be used to deconvolve the observed data cube from the PSF, although this will be addressed in a future project.

Acknowledgments

Based on data from the ESO science archive facility with DOI(s): https://doi.org/10.18727/archive/41. The authors acknowledge support from the Spanish Ministry of Science and Innovation through the Spanish State Research Agency (AEI-MCINN/10.13039/501100011033) through grants "Participation of the Instituto de Astrofísica de Canarias in the development of HARMONI: D1 and Delta-D1 phases with references PID2019-107010GB-100 and PID2022-140483NB-C21 and the Severo Ochoa Program 2020-2023 (CEX2019-000920-S).

References

[1] Bacon, R., Brinchmann, J., Richard, J., et al. (2015), A&A, 575, A75.

[2] Calderone, G., Nicastro, L., Ghisellini, G., Dotti, M., Sbarrato, T., Shankar, F., & Colpi, M. (2017), *Monthly Notices of the Royal Astronomical Society*, 472(4), 4051-4080.

[3] Esparza-Arredondo, D., García-Lorenzo, B., Acosta-Pulido, J.A., & Castro-Almazán, J. (2025), *in preparation*

[4] García-Lorenzo, B., Esparza-Arredondo, D., Acosta-Pulido, J. A., & Castro-Almazán, J. A. (2024), A&A, 687, A40.

[5] Kaspi, S., Smith, P. S., Netzer, H., Maoz, D., Jannuzi, B. T., & Giveon, U. (2000), *The Astrophysical Journal*, 533(2), 631–649.

[6] Kormendy, J. and Ho, L. C. (2013), *Annual Review of Astronomy and Astrophysics*, vol. 51, pp. 511–653.

[7] Padovani, P., Alexander, D. M., Assef, R. J., De Marco, B., Giommi, P., Hickox, R. C., Richards, G. T., Smolčić, V., Hatziminaoglou, E., Mainieri, V., & Salvato, M. (2017), *Astrophysics and Space Science Review*, 25(1), 2.

[8] Tokovinin, A. (2002), *PASP*, 114, 1156-1166.